Regular Article

MYELOID NEOPLASIA

Dysregulated signaling pathways in the development of CNTRL-FGFR1–induced myeloid and lymphoid malignancies associated with FGFR1 in human and mouse models

Mingqiang Ren, Haiyan Qin, Eiko Kitamura, and John K. Cowell

Georgia Regents University Cancer Center, Augusta, GA

Key Points

- CNTRL-FGFR1 induces AML and T-cell lymphoma in murine and human progenitor cells.

- Simultaneously targeting FGFR1, FLT3, KIT, and MYC synergistically induces cell growth inhibition in CNTRL-FGFR1–transformed cells.

Myeloid and lymphoid neoplasm associated with FGFR1 is an aggressive disease, and resistant to all the current chemotherapies. To define the molecular etiology of this disease, we have developed murine models of this disease, in syngeneic hosts as well as in nonobese diabetic/severe combined immunodeficiency/interleukin 2Rγ^{null} mice engrafted with transformed human CD34^{+} hematopoietic stem/progenitor cells. Both murine models mimic the human disease with splenohepatomegaly, hypercellular bone marrow, and myeloproliferative neoplasms that progresses to acute myeloid leukemia. Molecular genetic analyses of these model mice, as well as primary human disease, demonstrated that CNTRL-FGFR1, through abnormal activation of several signaling pathways related to development and differentiation of both myeloid and T-lymphoid cells, contribute to overt leukemogenesis. Clonal evolution analysis indicates that myeloid related neoplasms arise from common myeloid precursor cells that retain potential for T-lymphoid differentiation. These data indicate that simultaneously targeting these pathways is essential to successfully treating this almost invariably lethal disease. (*Blood*. 2013;122(6):1007-1016)

Introduction

Constitutive activation of FGFR1 kinase in hematopoietic stem cells (HSC) resulting from chromosome translocations involving 8p11 leads to myeloproliferative neoplasms (MPN) that inevitably progress to acute myeloid leukemia (AML) and is frequently accompanied by T- and B-cell lymphomas. Overall survival is poor due to resistance to current therapeutic regimens. The hallmark of FGFR1-related neoplasms is bilineage disease, in which tumor cells from both lineages harbor the chimeric FGFR1 fusion gene, suggesting a common stem/progenitor origin. *FGFR1* fuses to more than 11 partner genes,[1] such as ZMYM2-FGFR1, BCR-FGFR1, and CNTRL-FGFR1. Constitutive activation of FGFR1 is believed to be the primary initiation event that drives disease development, although its oligoclonal nature suggests other genetic events are required for progression.

We, and others, have developed syngeneic murine models of FGR1-related neoplasms[2-5] that mimic the human disease, although they do not apparently progress to AML, despite development of lymphomas. FGFR1 fusion to the centrosomal CNTRL protein[6,7] is one of the more common rearrangements, and we have now developed a syngeneic mouse model that develops MPN that rapidly progresses to AML as seen in the human disease.[6-8] Unlike previous models, CNTRL-FGFR1–transduced bone marrow (BM) shows a long (6 to 10 months) latency before development of MPN and, although rarely animals develop T- and B-lymphomas, the majority develop

AML. Thus, the CNTRL-FGFR1 model offers an opportunity to study the events in HSC that mark the progression to AML.

To determine whether the same progression profile for CNTRL-FGFR1 disease could be recapitulated in human cells, we have also developed a model for this disease using CD34^{+} human stem/progenitors maintained in nonobese diabetic/severe combined immunodeficiency/interleukin (IL)2R^{null} (NSG) immunocompromised mice. Using a retroviral transduction and transplantation procedure, we show that the *CNTRL-FGFR1* gene induces concurrent AML and T-cell leukemia/lymphoma in the human cells, which is accompanied by aberrant transcription of multiple lineage-specific gatekeeper genes that can regulate the commitment of progenitor cells into either a myeloid, T-cell or bilineage disease. On occasion, the AML transdifferentiated into T-cell lymphoblastic lymphoma (T-LBL) during serial transplantation.

Methods

Cloning and sequencing of the *CNTRL-FGFR1* fusion cDNA

Complementary DNA (cDNA) from BM RNA from a patient with a CNTRL-FGFR1 rearrangement[9] was the kind gift from Dr Matsui. The polymerase

---

chain reaction (PCR) fragment containing the full-length fusion gene was amplified using fidelity Taq DNA polymerase (Invitrogen) using the following primers with the respective restriction enzyme adaptor: forward EcoRI-CEP, 5′-TCGACGAATTCATAATGCAGCATTTA; reverse XhoI, 5′-AAT GGCTCG AGCAGTCAGCGGCGT TT using standard PCR conditions. The PCR product was then subcloned into the EcoRI/Xho sites of the murine stem cell virus vector (MIEG3).[10] Sanger sequencing confirmed the sequence of final CNTRL-FGFR1 fusion gene.

Retroviral transduction and transplantation

The production of retroviral particles, retroviral transduction of BM, and transplantation was performed as described previously.[3] Anonymized human cord blood cells were obtained from the Georgia Health Sciences University Cord Blood Bank under an approved institutional review board protocol (#1002143); approval was also obtained from the Georgia Health Sciences University institutional review board for these studies. Informed consent was obtained according to the Declaration of Helsinki. CD34^{+} cells were isolated using the EasySep Cord Blood CD34 Positive Selection Kit (StemCell Technologies) following the manufacturer's protocol, and expanded in StemSpan SFEM medium (StemCell) supplemented with recombinant human cytokines: low-density lipoprotein 10 μg/mL, Flt-3 100 ng/mL, stem cell factor 100 ng/mL, thrombopoietin 50 ng/mL, IL-3 20 ng/mL, and IL-6 20 ng/mL (R&D Systems). After 24 hours of prestimulation, CD34^{+} cells were transduced as described previously[11] and transplanted into NSG mice.

Analysis of diseased mice

Mice that received transplants were evaluated daily for symptoms of disease as described previously[3] to determine progression of the disease. During the course of this monitoring, peripheral blood (PB) samples were obtained from the tail veins to analyze the green fluorescent protein positive (GFP^{+})/CD45^{+} cells periodically after transplantation except as otherwise noted. For secondary and tertiary recipient animals, a range of 2.5 to 3 million cells from BM and/or spleen of primary or secondary recipients was transplanted into individual recipients by tail-vein injection. All animal experiments were carried out under protocols approved by the Institutional Animal Care and Use Committee of the Georgia Health Sciences University.

Flow cytometry analysis and stem cell sorting

Details of the specific conjugated antibodies used for flow cytometric analysis were as described previously.[3,11]

Cell culture and proliferation assays

All cell lines were cultured in RPMI (Invitrogen) with 5% fetal bovine serum (Hyclone), at 37°C in 10% CO_2. For drug treatments, 40 000 cells/well were seeded in 96-well plates and incubated overnight, then treated with the either dimethylsulfoxide (control) or the drugs indicated in the "Results" section at concentrations defined by the experiments. Cell viability was determined as described.[11]

Primary leukemic spleen cell treatment

Leukemic cells were isolated from BM and spleens of leukemic mice (n = 3) by flushing RPMI medium through the long bones or by smashing the spleen in cell strainers. In vitro, spleen cells were cultured in RPMI medium supplemented with 20% fetal calf serum and treated with JQ1 and ponatinib for 48 hours at the concentrations presented in the respective figures.

Molecular and immunoglobulin heavy-chain rearrangement analyses

The PCR primers and conditions used in the molecular analyses are described elsewhere[3,12] or in supplemental Table 4. Western blot analysis of CNTRL-FGFR1 fusion protein expression was performed using standard protocols with the respective primary antibodies as described.[11,12] Comparative

genomic hybridization (CGH) was performed using Agilent SurePrint G3 Mouse CGH 4 × 180 K microarrays (Agilent) as described previously.[4]

The VDJ rearrangements of the immunoglobulin heavy chain has been described in detail previously.[13] Amplification of complete DJH rearrangements was performed using 2 upstream degenerate primers (DFS, DQ52) and one reverse primer (JH4). All 3 primers were used in a single reaction to detect rearrangements from DJH1 to DJH4.

Whole-transcriptome cDNA library construction and sequencing

cDNA libraries were generated using the Illumina TruSeq RNA Sample Preparation kit following the manufacturer's instructions. Briefly, messenger RNA was isolated by oligo-dT beads and fragmented by adding Elute, Prime and Fragment Mix (provided by Illumina). Fragmented messenger RNA was converted to cDNA using First Strand and Second Strand master mixtures (Illumina). Purified cDNA was subjected to end repair, A-tailing, and adapter ligation. The adapters contain index sequences to allow for Illumina multiplex sequencing. The cDNA template was amplified using 15 cycles of PCR for 10 seconds at 98°C, 30 seconds at 60°C, and 30 seconds at 72°C using a PCR master mixture (Illumina) and purified by AMPure XP beads (Agencourt). The quality of the resulting cDNA libraries was assessed using a Bioanalyzer DNA 1000 chip (Agilent) and quantified by quantitative PCR (Bio-Rad). The cDNA libraries were sequenced using paired end Illumina Hiseq2000 protocols (50 cycles).

Data processing analysis

The Illumina sequencing pipeline version 1.8 was employed for transferring raw images to base calls, generating sequence reads, and de-multiplexing the reads. The generated FASTQ files were imported to CLC Genomics Workbench and aligned to the mouse genome NCBI37/mm9. The transcript expression levels (Gene Expression Omnibus accession number GSE48048) were determined in terms of number of reads per kilobase per million and compared between sorted normal myeloid (Gr1^{+}Mac1^{+}) cells and sorted leukemic myeloid cells (B220[+]Gr1^{+}Mac1^{+}). The gene cluster and gene set enrichment analyses were described previously.[12]

Results

CNTRL-FGFR1 induces transformation of BaF3 cells

The CNTRL-FGFR1 cDNA was generated from an FGFR1-related leukemia[9] and cloned into the MIEG3 vector (Figure 1A). IL-3–dependent murine BaF3 pro-B cells infected with CNTRL-FGFR1 grew continuously in the absence of IL-3 compared with MIEG3-infected cells, which died (Figure 1B-C). Western blot analysis demonstrated high-level expression of the fusion protein in CNTRL-FGFR1–infected cells (Figure 1D) showing its transforming ability.

CNTRL-FGFR1 induces leukemia and lymphoma in a syngeneic mouse model

BM cells from 5 normal male BALB/c donors were transduced independently with MIEG3-CNTRL-FGFR1; subsequently, each of the 5 samples was transplanted into 2 lethally irradiated (850 cGy), syngeneic female recipients. Two mice died of radiation toxicity but the remaining 8 recovered their white blood cell count over 2 weeks following transplantation, demonstrating successful engraftment. Seven to 10 months posttransplantation, white blood cell counts increased and blast cells appeared in all 8 recipients (supplemental Figure 1A). Increased GFP^{+} cells were seen in the PB from most primary recipients (data not shown). On autopsy, 4 out of 8 mice demonstrated enlarged lymph nodes and/or thymuses (supplemental Figure 1B and supplemental Table 1) and 5 out of
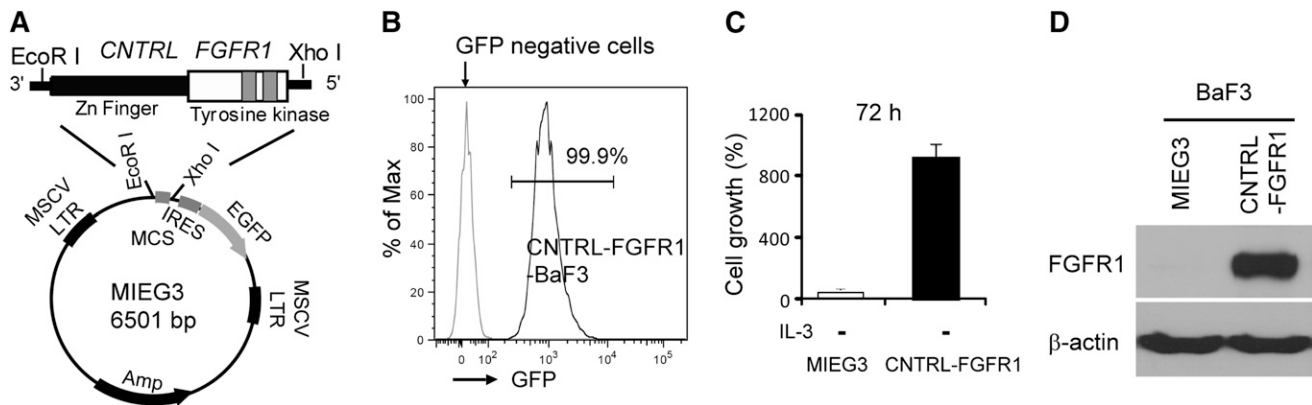
Figure 1. The CNTRL-FGFR1 fusion kinase induces BaF3 cell transformation. (A) Scheme for construction of the MIEG3-CNTRL-FGFR1. (B) Flow cytometry analysis shows that almost all BaF3 cells transformed by CNTRL-FGFR1 are viable and express GFP after withdrawal of IL-3. (C) Cell proliferation assays demonstrate increased IL-3–independent growth of CNTRL-FGFR1-BaF3 cells. (D) Western blot analysis shows the presence of the CNTRL-FGFR1 fusion protein in stably transformed BaF3 cells.

8 showed splenomegaly (Figure 2A). For the T-lymphomas, the mean latency was 189 days and 265 days for AML, which is significantly longer than the BCR-FGFR1[4] or ZMYM2-FGFR1 models (Figure 2B).[3]

Histological analyses demonstrated hypercellularity in the marrow from the sternum (supplemental Figure 1D). Leukocyte infiltration was often seen in organs such as in the spleens, livers, lungs, and kidneys (supplemental Figure 1D). Enlarged kidneys were seen in 20% of the primary recipients, and infiltrating leukocytes had destroyed the normal follicular architecture of the spleen (supplemental Figure 1D).

CNTRL-FGFR1 induces both AML and T-cell leukemia/lymphoma

Immunophenotype analysis of cells from the BM, spleen (SP), and PB of primary recipients revealed at least 2 different lineages. Two of 8 mice (25%) demonstrated enlarged lymph nodes and thymuses (supplemental Figure 1A). Flow cytometry showed a dominant $GFP^+CD4^+CD8^+$ immunophenotype in cells from BM, PB, SP, and thymus from these mice (Figure 2C), suggesting T-cell leukemia/lymphoma. More than 95% of thymocytes were GFP^+ (Figure 2C), indicating that the thymuses were involved in the abnormal T-cell development. Rare $GFP^+Mac1^+Gr1^+$ and GFP^+B220^+ cells were seen in the BM, SP, and PB (Figure 2C) of these mice. One cell line (designated CEP2A) was isolated from the BM of 1 of these 2 mice, and flow cytometry analysis indicated a T-cell origin, with a GFP^+CD4^+ or $GFP^+CD4^+CD8^+$ immunophenotype (supplemental Figure 2).

The majority (6/8) of primary recipients predominantly developed myeloid leukemia, with a $B220^+Gr1^+Mac1^+$ immunophenotype in BM, PB, and SP (Figure 2D), suggesting they are immature blast cells and indicating that these mice, similar to CNTRL-FGFR1 patients, had developed AML. Interestingly, AML cells from a CNTRL-FGFR1 patient reported recently also coexpressed B-cell lineage markers.[14] The $B220^+Gr1^+Mac1^+$ cells were both GFP^+ and GFP^-, suggesting inactivation of GFP in subpopulations, as we observed previously.[4] Pathological analysis of this group of mice showed hemorrhage in their chests, together with increased blood volume (supplemental Figure 1C), that their spleens were slightly larger than controls, and that their thymuses were almost undetectable (supplemental Figure 1C and supplemental Table 1). Surprisingly, another cell line (designated CEP5A), isolated from the BM of 1 of these mice, expressed a $GFP^+CD8^+CD25^+$ immunophenotype, suggesting a T-lineage origin (supplemental

Figure 2). CEP5A, however, showed a germ line configuration of the *Tcrb* gene (Figure 3B), suggesting that these cells may have *trans*-differentiated from a myeloid progenitor clone.

CNTRL-FGFR1 disease is transplantable and originates from oligo- or monoclonal stem/progenitor cells

CNTRL-FGFR1 clearly induces bilineage disease, suggesting a stem/progenitor cell origin. In a second series, BM cells from the primary leukemic mice (n = 6) were transplanted into secondary recipients (n = 18), which developed leukemia/lymphoma (median = 171 days posttransplantation), with a latency similar to the primary recipients (Figure 3A). Although 1 primary recipient (#3), showed a myeloid to T-cell leukemia/lymphoma lineage switch in the second BM transplantation recipient (supplemental Figure 3), all of the other secondary recipients developed AML, consistent with their primary recipients. Analysis of *Tcrb* rearrangement in the T-cell lymphomas demonstrated oligo- or monoclonal disease in both the primary and secondary mice (Figure 3B), indicating that additional genetic changes are required for overt T-cell leukemia/lymphoma development. Because the AML cells expressed B220, they potentially originated from progenitor B cells, although it is also possible that this antigen is expressed in a non-lineage–specific way. $B220^+Gr1^+Mac1^+$ AML cells were sorted from 2 CNTRL-FGFR1 mice, and normal myeloid cells ($Gr1^+Mac1^+$) and B cells ($B220^+CD19^+$) were sorted from 3 normal BALB/c mice. Reverse transcription-polymerase chain reaction (RT-PCR) analysis clearly showed that the AML cells as well as the normal myeloid cells did not express B-cell–specific genes *Ebf1*, *Pax5*, and *Vpreb1*[15,16] (Figure 3C). Consistently, the AML cells did not contain *IgH* rearrangements, compared with the normal B cells ($Gr1^-Mac1^-B220^+$) sorted from the matched disease mice, or myeloid cells ($Gr1^+Mac1^+$) sorted from the normal BALB/c mice (Figure 3D). Thus, the murine AML cells apparently originated from myeloid progenitor cells, although they expressed surface B220.

Tcra deletion and *Notch1* activation is associated with T-cell leukemia/lymphoma development

Deletion of the T-cell receptor α (*Tcra*) gene,[3] and activating mutations of *Notch1*,[12] were demonstrated during development of T-LBL in ZMYM2-FGFR1 mice. Because the T-LBL induced by CNTRL-FGFR1 shows almost the same immunophenotype as that induced by ZMYM2-FGFR1, we investigated whether this was also the case for CNTRL-FGFR1. CGH profiles showed trisomies
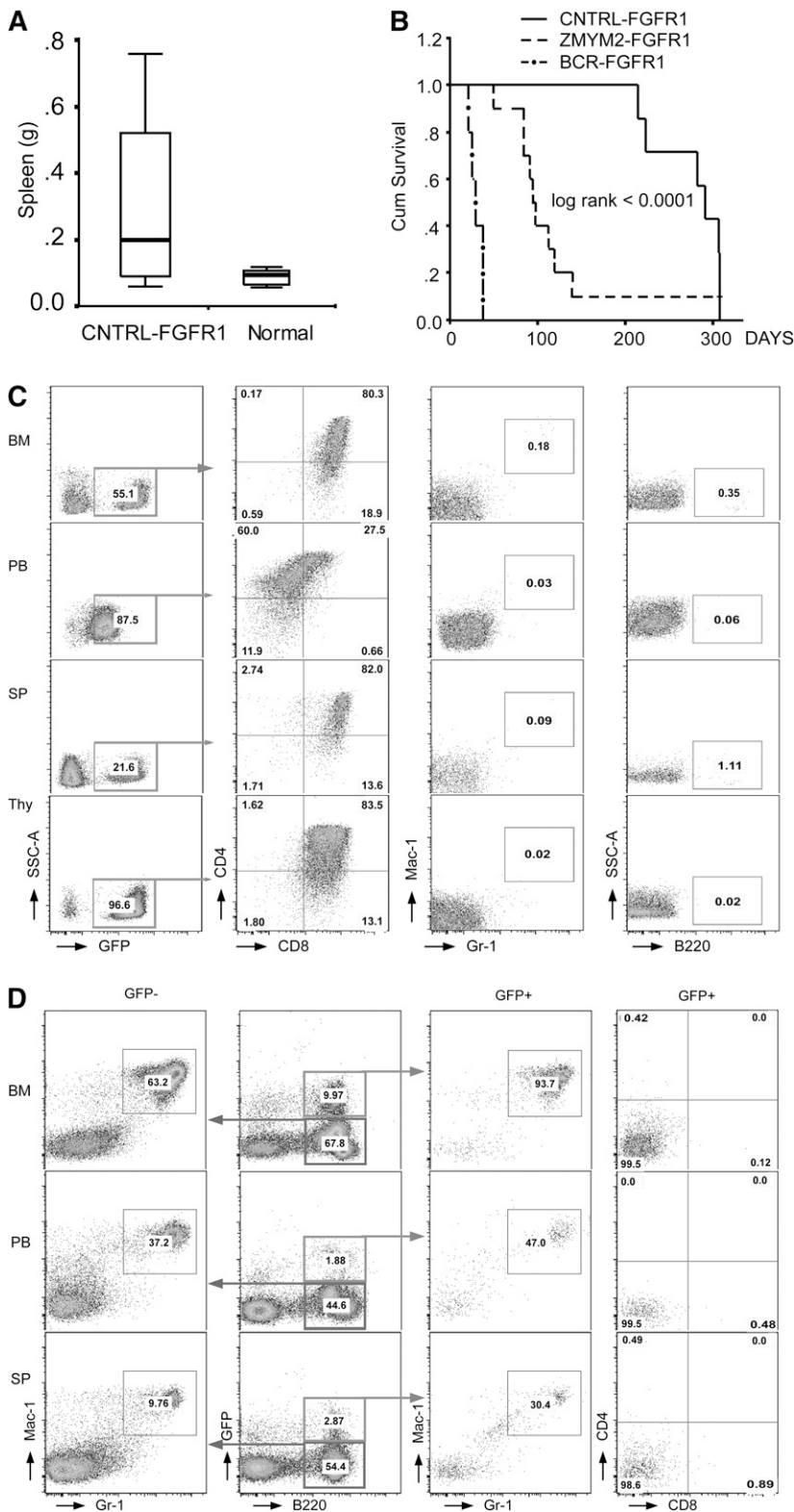
Figure 2. Phenotypic analysis of CNTRL-FGFR1 transduced and transplanted mice. (A) Comparison of splenic weight between leukemic and normal mice. (B) Comparison of survival from 3 chimeric BM transduction and transplanted mouse models. (C) Flow cytometric analysis (see "Methods") of cells in BM, PB, SP, and thymus (Thy) from 2 mice with T-LBL shows a CD4$^+$CD8$^+$ phenotype. (D) Flow cytometry analysis shows that cells from a representative mouse that developed AML have a B220$^+$Gr1$^+$Mac1$^+$ immunophenotype in both GFP$^+$ and GFP$^-$ cell populations.

for chr7, chr10, and chr15, together with a deletion of the *Tcra* locus on chr14 (Figure 4B) in the CEP2A and CEP5A cell lines (Figure 4A) and ZMYM2-FGFR1–containing ZNF112 cells.[12] The *Tcra* deletion was confirmed using gene-specific PCR analysis (Figure 4C) as well as by flow cytometric analysis using the Tcra V2 antibody, which showed loss of cell surface Tcra receptor (Figure 4D). Deletion of *Tcra*, however, in itself is not sufficient to

induce T-LBL as evidenced by *Tcra*-null mice,[17,18] suggesting additional genetic or epigenetic changes are required. Western blot analysis for activated Notch1 (Val1744) in CNTRL-FGFR1–induced T-lymphoma clearly showed that both lymphoma samples and established cell lines carried activated Notch1 (Figure 4E) as seen in ZMYM2-FGFR1 mice.[12] Genomic PCR analysis demonstrated that aberrant activation of *Notch1* is due to deletions in the promoter
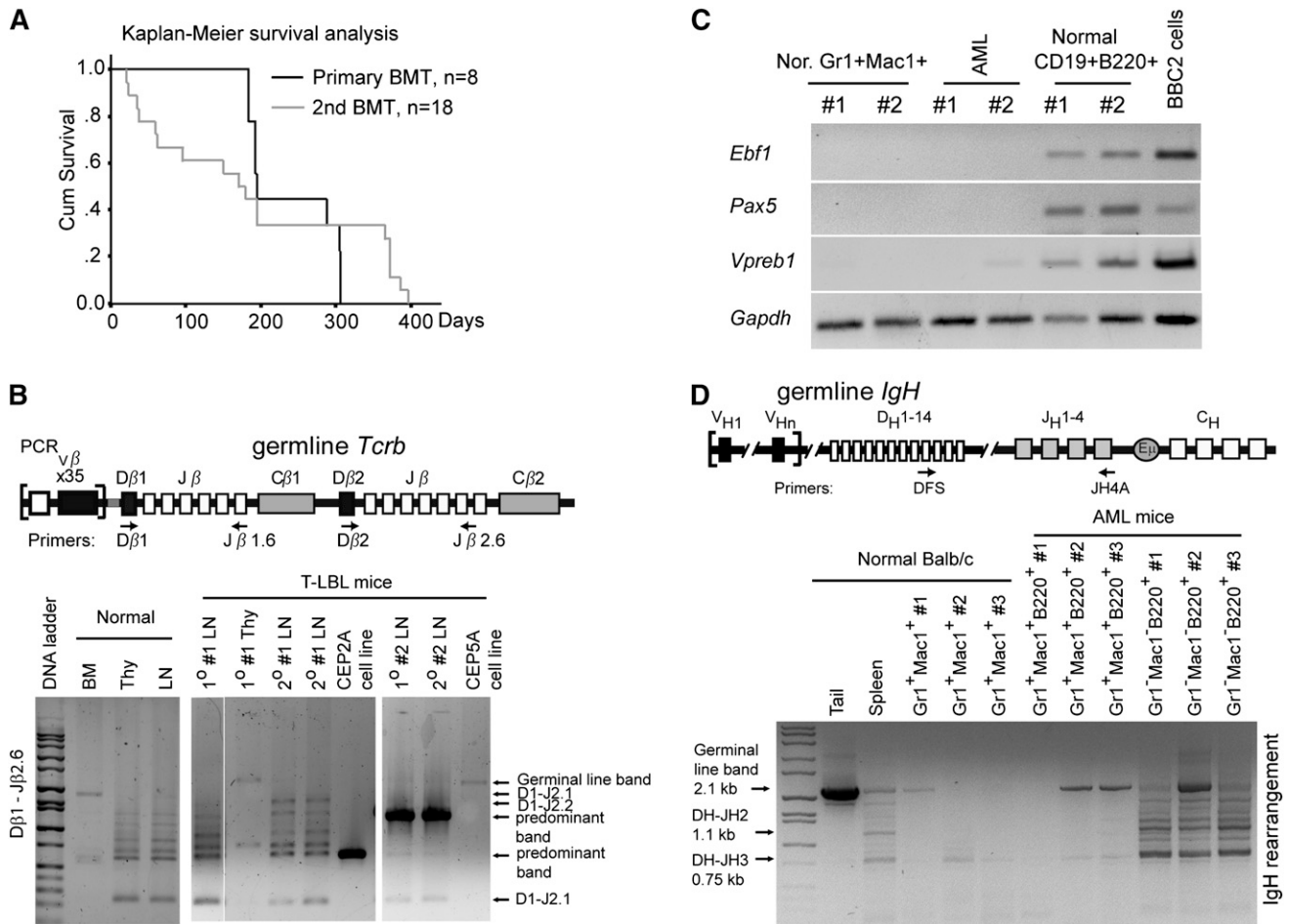
Figure 3. CNTRL-FGFR1 neoplasms are transplantable and originate from oligo- or monoclonal hematopoietic stem/progenitor cells. (A) Kaplan-Meier analysis of primary and secondary recipients shows no significant difference between the primary and secondary transplants. (B) Schematic representation showing the relative location of the PCR primers used to analyze the *Tcrb* locus (top). Gel electrophoresis of PCR products shows DJ arrangement of *Tcrb* in 2 representative, serially transplanted CNTRL-FGFR1 mice (bottom). DNA from BM displays 1 large band reflecting no rearrangement. DNA from normal Thy and lymph node (LN) shows several smaller bands resulting from rearrangements. DNA from Thy and LNs from 2 leukemic mice (#2, #5) shows oligo- or monoclonality. Specifically, DNA from 2 cell lines (CEP2A and CEP5A) shows only 1 predominant band (arrow), indicating that these lymphoma cells were monoclonal. (C) RT-PCR analysis shows the specific transcriptional levels of B-lineage genes in sorted myeloid cells (Gr1$^+$Mac1$^+$) or B cells (B220$^+$CD19$^+$) from normal (Nor) BALB/c mice as well as in sorted AML cells (Gr1$^+$Mac1$^+$ B220$^+$) from 2 leukemic mice. The B-lymphoid cell line BBC2 is shown as a positive control. (D) Genomic PCR analysis of IgH rearrangement showing the germline configuration in DNA from the tail and polyclonal rearrangements in the B cells sorted from 3 normal BALB/c mouse splenocytes. The B220$^+$Gr1$^+$Mac1$^+$ AML cells have the same pattern as normal Gr1$^+$Mac1$^+$ myeloid cells.

region (Figure 4F) as previously described.[12] Consistently, cell growth was significantly inhibited (Figure 4G) by the DAPT or CompE Notch1 inhibitors.[19] Thus, constitutive activation of *Notch1* together with *Tcra* deletion cooperate with *CNTRL-FGFR1* to promote T-lineage lymphomagenesis, providing a molecular basis for T-LBL development in the CNTRL-FGFR1 mouse model.

Aberrant gene expression related to myeloid cell development contributes to CNTRL-FGFR1–induced AML

To characterize gene expression changes in AML induced by CNTRL-FGFR1, we used RNA-seq analysis of sorted Mac$^+$Gr1$^+$ B220$^+$ AML cells (n = 2) from the SP and BM of leukemic mice as well as sorted Mac$^+$Gr1$^+$ myeloid cells (n = 3) from normal mice. Unsupervised analysis of the datasets showed a remarkable difference between normal (Gr1$^+$Mac1$^+$) and leukemic (Mac$^+$Gr1$^+$ B220$^+$) myeloid cells (Figure 5A). Gene Set Enrichment Analysis (Figure 5B) and leading-edge analysis (Figure 5C), suggested that Mac$^+$Gr1$^+$B220$^+$ cells have the potential to differentiate into either myeloid or T-cell, but not a B-cell lineages. Quantitative RT-

PCR analysis of lineage-specific genes[20-23] showed increased expression of *Flt3, Gfi1, and Kit* related to early myeloid-lineage commitment, whereas genes related to myeloid differentiation, *Irf8, Klf4, Csf1r, Myc*, and *Spi1,* were decreased compared with normal myeloid cells (Figure 5D). Quantitative RT-PCR also confirmed that the *Cd3e* and *Lmo2* T-cell–specific genes were markedly increased in AML cells (Figure 5D). Consistent with their molecular signature, the disease had transitioned from a myeloid to a T-cell lineage. Transplantation of BM cells from 1 (#3) primary recipient with AML into 3 secondary recipients (supplemental Figure 3A) showed that only 1 secondary recipient developed AML similar to its donor mouse, and the other 2 developed T-cell leukemia/lymphoma (supplemental Figure 3B).

CNTRL-FGFR1 exclusively promotes human AML development in mice engrafted with transduced human CD34$^+$ progenitor cells

To determine whether CNTRL-FGFR1 also induces disease in human cells, we developed an immunodeficient mouse model engrafted with either CNTRL-FGFR1 or control MIEG3-infected human
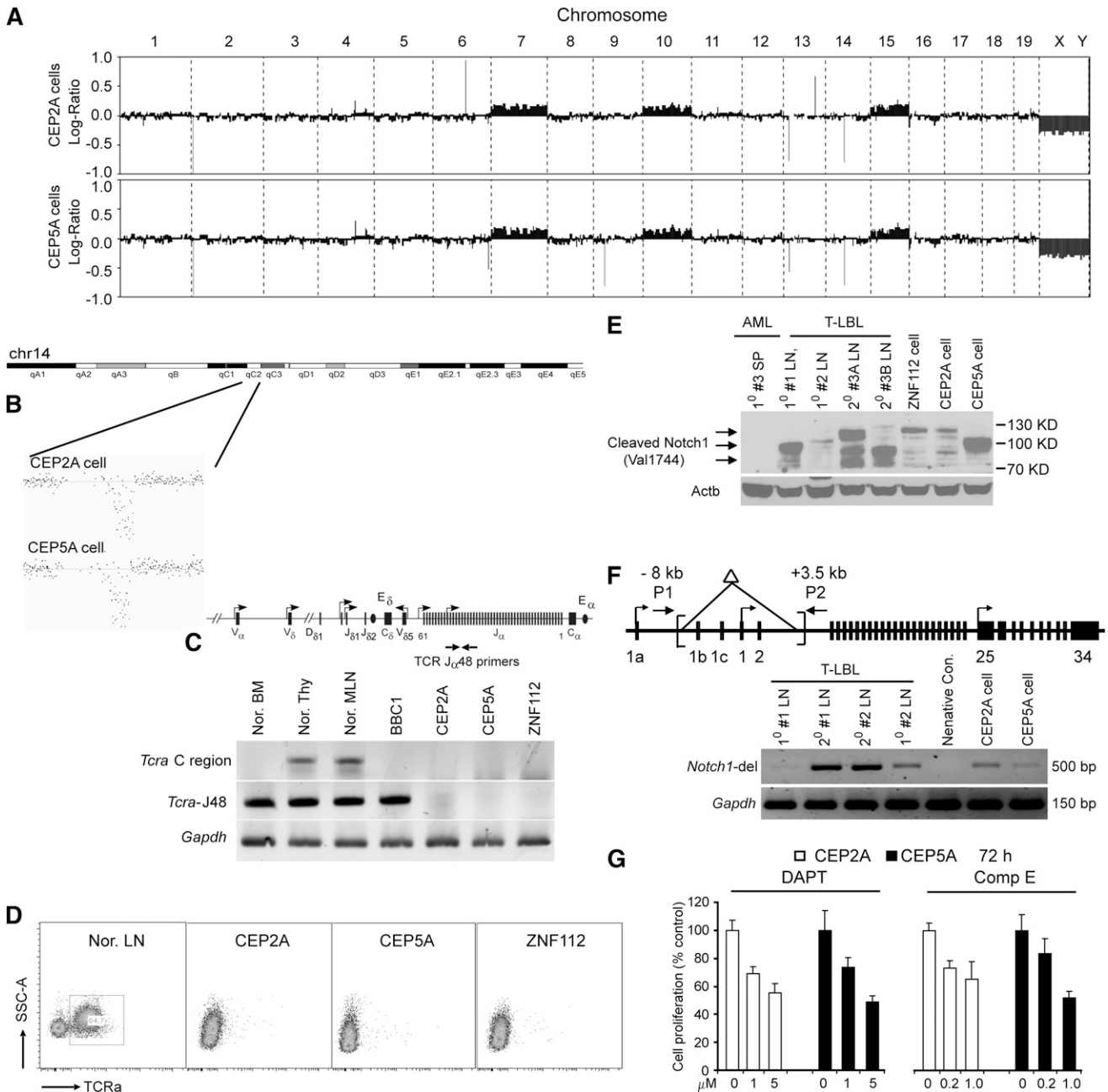
Figure 4. Mutational activation of *Notch1* and deletion of *Tcra* are etiologically associated with the development of T-cell leukemia/lymphoma. (A) Array CGH analysis of CEP2A (top) and CEP5A (bottom) cells shows almost identical chromosome changes in the 2 cell lines, including 14qC2 segmental loss as well as gain of chr7, chr10, and chr15. (B) Detailed view of murine *Tcra* deletion in both CEP2A and CEP5A cell lines. (C) Genomic PCR confirms loss of *Tcra* in the CEP2A and CEP5A cells. (D) Flow cytometric analysis reveals that both CEP2A and CEP5A cells are negative for cell-surface Tcra. (E) Western blot analysis, using antibodies against the activated Notch1 (Val 1774 antibody, Cell Signaling Technologies), showing that activated Notch1 (different bands resulting from different truncating mutations) is present in LN isolated from the primary (1°) and secondary (2°) T-LBL mice compared with 3 murine FGFR1-related neoplasm cell lines. A spleen sample from #3 AML mouse is used as a negative control. (F) Schematic of the *Notch1* gene showing the relative locations of the primers used to analyze the deletion mutants (top). A 5′ deletion (brackets) creates a 500-base pair fragment using the P1/P2 primers, as shown in LN from different T-LBL mice. In normal cells, the wild-type 11.5-kb fragment cannot be amplified.[12] (G) γ-Secretase inhibitors DAPT and Comp E significantly inhibit CEP2A and CEP5A cell growth in vitro at micromolar concentrations.

CD34$^+$ cells as described[11] (Figure 6A). These transplanted mice were monitored for disease progression for blast cells in blood smears. After ~7 months, increased leukocyte and blasts were observed in CNTRL-FGFR1 mice (n = 9) (supplemental Figure 4A). All of these mice developed leukemia within 15 months, whereas the MIEG3 control mice did not (n = 4) (Figure 6B and supplemental Table 2). Similar to the BABL/c model, the CNTRL-FGFR1-NSG mice showed splenohepatomegaly (supplemental Figure 4A), hypercellular BM, and leukocyte infiltration into several

organs (supplemental Figure 4B). Human CD45$^+$ leukocytes from CNTRL-FGFR1-NSG mice were either GFP^{dim} or GFP$^-$ (supplemental Figure 4C). RT-PCR analysis across the *CNTRL-FGFR1* breakpoint confirmed the presence of the fusion gene in the GFP$^-$ splenocytes (supplemental Figure 4C). Flow cytometry analyses showed that >95% of the human CD45$^+$ cells were also CD13$^+$. Thus, the CNTRL-FGFR1-NSG mice developed human AML, based on their immunophenotype and morphology (Figure 6C and supplemental Figure 4A). Interestingly, 5% to 20% of the
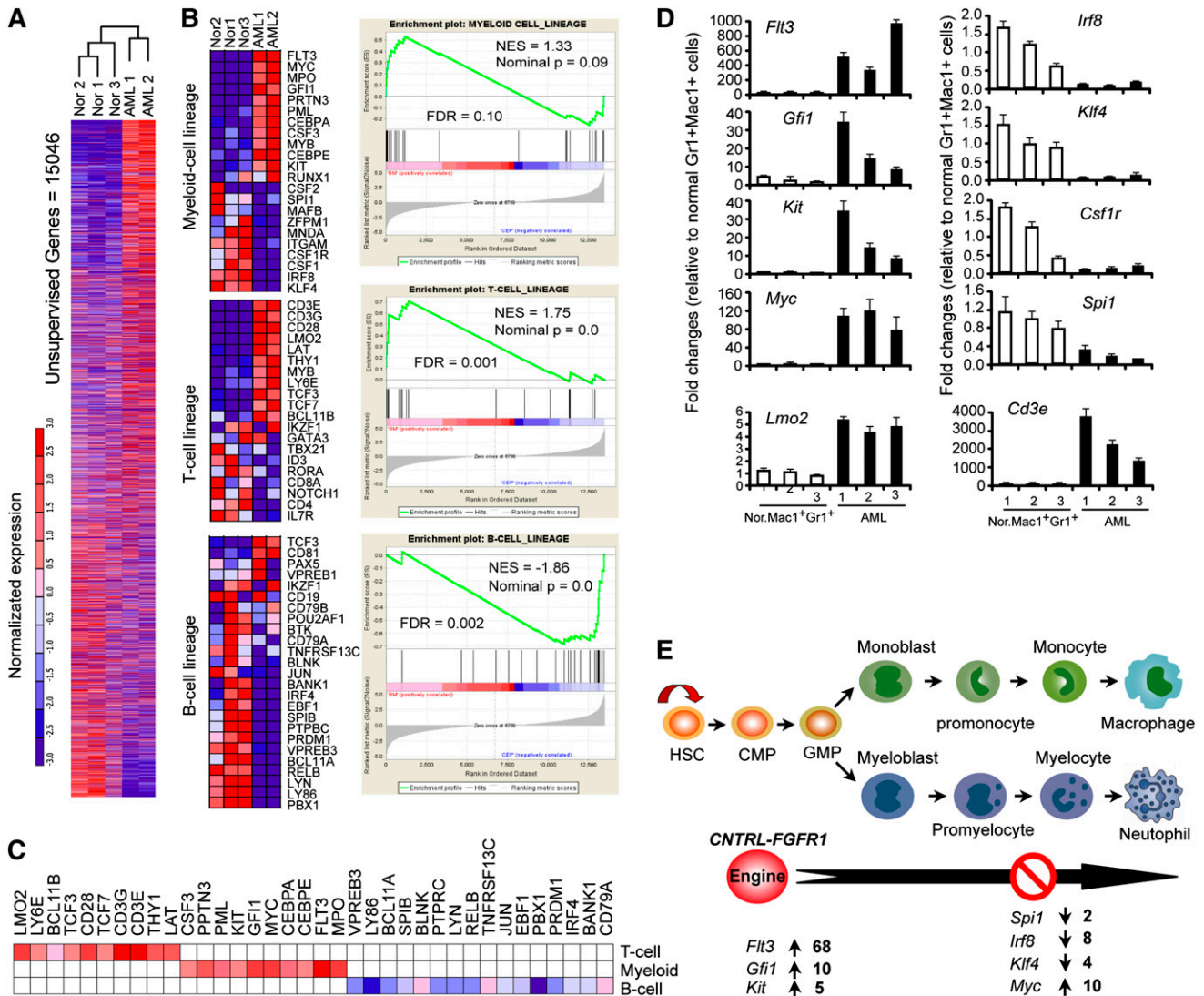
Figure 5. Gene expression analysis by RNA-seq demonstrates dysregulation of multiple genes associated with myeloid cell development. (A) Hierarchical cluster analysis generated by Euclidean distance and pairwise complete-linkage analysis of unsupervised RNA-seq data. (B) Heat map (left) and Gene Set Enrichment Analysis (right) show genes related to myeloid and T-lymphoid cell development are up-regulated (red) in sorted AML cells (B220$^+$Gr1$^+$Mac1$^+$) compared with sorted normal myeloid cells (Gr1$^+$Mac1$^+$) from normal BALB/c mice ($P < .05$). (C) Leading-edge analysis of RNA-seq data sets demonstrates gene expression patterns in leukemic cells characteristic of both myeloid and T-lymphoid lineage cells. (D) Quantitative RT-PCR analysis confirms the transcription level changes for selected genes in AML cells measured by RNA-seq shown in (B). (E) Schematic summary of differentially expressed genes related to stages of myeloid development.

CD45$^+$ cells also showed a CD4$^+$/CD8$^+$ immunophenotype (Figure 6C). To further investigate whether AML in CNTRL-FGFR1-NSG mice and human CNTRL-FGFR1 patients have a similar gene expression pattern as that seen in CNTRL-FGFR1-BALB/c mice, we used quantitative RT-PCR to compare gene expression levels between spleen cells from CNTRL-FGFR1-NSG and MIEG3-NSG mice. We also compared the gene expression from the CNTRL-FGFR1 patient from whom the *CNTRL-FGFR1* cDNA was cloned and 2 normal human PB mononuclear cell samples. The overall gene expression patterns were similar to those seen in the CNTRL-FGFR1 BALB/c mice, except for upregulation of *CSF1R* expression (Figure 6D). High-level expression of *FLT3*, *GFI1*, and *MYC*, which have been shown in AML patients,[24-26] was confirmed in CNRTL-FGFR1-NSG mice by western blot (Figure 6E) and flow cytometry analysis (Figure 6F). To determine whether overexpression of this panel of genes was functionally important in AML development, we used the ponatinib[27]

tyrosine kinase inhibitor (targeting FLT3, KIT, and FGFR1) and the JQ1 MYC inhibitor[28] to treat primary AML cells isolated from CNTRL-FGFR1 mice. The combination of these drugs generated a synergistic growth inhibition in primary splenocytes from 3 diseased mice (#3, #4, and #7), but almost no effect on normal human PB mononuclear cells (Figure 6G). We further treated human KG-1 AML cells (carrying FGFR1OP2-FGFR1) with these 2 drugs, either alone or combination. Cell growth of KG-1 was synergistically inhibited by ponatinib and JQ1 at nanomolar concentrations, compared with AML U937 cells (showing no FGFR1 or MYC abnormalities) and HL-60 cell (harboring MYC amplification) (Figure 6H). Thus, these studies demonstrate that CNTRL-FGFR1 predominately transforms human CD34$^+$ progenitor cells into AML, mediated by deregulation of multiple key genes related to myeloid cell development and differentiation, and simultaneously targeting some of these genes can inhibit AML cell growth.
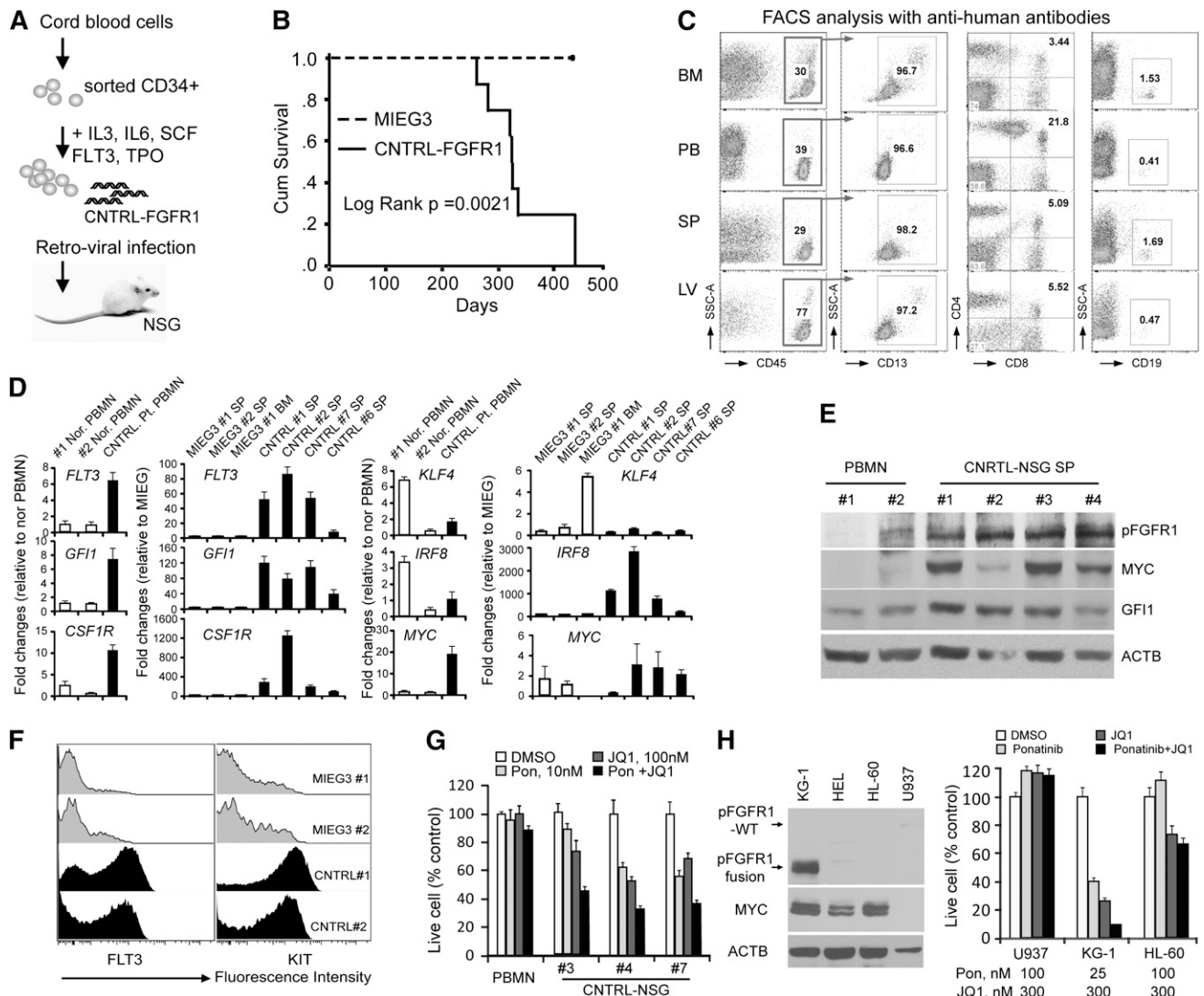
Figure 6. Human CD34^{+} progenitor cells transduced and xenotransplanted in NSG mice develop into AML. (A) Schematic representation of the experimental approach to generate the human CD34^{+} progenitor mouse model carrying the *CNTRL-FGFR1* fusion gene. (B) Kaplan-Meier survival analysis of primary recipients following engraftment of either the MIEG3 control vector or CNTRL-FGFR1-transduced human CD34^{+} progenitor cells. (C) Representative flow cytometry analysis of BM, PB, SP, and liver (LV) cells from a primary recipient mouse. (D) Quantitative RT-PCR analysis shows the comparison of gene expression levels in CNTRL-FGFR1 mice (CNTRL) and 1 CNTRL-FGFR1 patient compared with an MIEG3-NSG (MIEG3) mouse and normal healthy human PB mononuclear cells (Nor. PBMN), respectively. (E) Western blot analysis shows the gene expression levels of activated FGFR1, MYC, and GFI1 in leukemic mouse spleens compared with normal human PBMN. (F) Flow cytometry analysis of FLT3 and KIT expression on the cell surface from the CNTRL-FGFR1-NSG (CNTRL) and control MIEG3-NSG (MIEG3) mice. (G) Cell viability assays show the synergistic effect of ponatinib (Pon) and JQ1 on cell growth inhibition in different primary leukemic mouse splenocytes and normal PBMN cells. (H) Western blot analysis shows the MYC, FGFR1, or FGFROP2-FGFR1 fusion protein levels in 4 human AML cell lines (left). Cell viability assays show the synergistic effect of Pon and JQ1 on cell growth inhibition is only seen in KG-1 cells that carry an FGFR1 rearrangement (right).

Discussion

Understanding the etiology of stem cell–derived leukemias and lymphomas can be difficult in human disease and frequently requires reconstruction of events based on the end-stage phenotype. Mouse models as described here faithfully recapitulate the human disease; however, they can follow the progression of the disease in more detail. To our knowledge, both the BALB/c and the human CD34^{+} xenotransplanted NSG models are the first that describe successful creation of CNTRL-FGFR1–induced neoplasms. Consistent with the human disease, both mouse models concurrently developed bi- or multiple-lineage disease. The development of these mouse models provides a significant step forward, not only in understanding the

molecular etiology of this disease, but also for defining treatment regimens that can be evaluated in preclinical trials. The availability of robust mouse models for preclinical trials is particularly important because FGFR1-related neoplasms are rare and it will be challenging to recruit large numbers of patients for clinical trials. The evaluation of customized therapies for treatment of this disease, therefore, will rely on these mouse models.

Of the reported cases of FGFR1-related neoplasms so far,[6,8,14,29] 16 carry the *CNTRL-FGFR1* rearrangement (supplemental Table 3). Of these cases, 11 either presented initially with the AML or subsequently transformed to AML, and 7 out of 15 concurrently developed myeloid and T-cell leukemia. Only 1 patient presented with AML and B-cell leukemia,[9] although approximately 77% of cells in the BM were positive for the CD3 T-cell marker.[9] In the mouse models,

the majority (6 out of 8) of primary CNTRL-FGFR1 disease in the BALB/c mice and 100% (9/9) of the CNTRL-FGFR1 NSG mice developed AML (supplemental Tables 1 and 2). Consistent with the human disease, 2 out of 8 of the primary CNTRL-FGFR1 BALB/c mice presented predominantly with T-cell leukemia/lymphoma and 4/9 CNTRL-FGFR1 NSG mice presented with AML and T-cell leukemia. The proportion of GFP^{+}B220^{+} cells present in BALB/c mice (Figure 2D) and CD45^{+}CD19^{+} cells in NSG model mice (Figure 6C), however, was only ~1%, so these leukemic B cells represent only a small subpopulation. Together, these observations demonstrate that both of the models we have developed closely mimic the human FGFR1-related disease.

In both mouse models, the long latency before leukemogenesis implies that other cooperating events are required for AML development. Indeed, we found that activating Notch1 mutations and deletions of *Tcra,* are involved in the development of the T-cell leukemia/lymphomas (Figure 4), which we also found in the ZMYM2-FGFR1 mouse model.[3,12] RNA-seq analysis demonstrated that many genes known to be related to myeloid cell development were dysregulated in the presence of the chimeric *CNTRL-FGFR1* gene. Importantly, these gene expression changes were identified in the syngeneic BALB/c-mouse model, the CD34^{+} NSG human-mouse model, and in primary cells from a patient with FGFR1-related neoplasms, which reinforces the representative nature of the mouse models for designing therapeutic strategies. As a result of this genetic analysis, it appears that the chimeric FGFR1 fusion kinase promotes expansion of the stem cell population, and that increased expression of *FLT3*, *GFI1*, and *KIT* promotes transformation of HSCs committed to a myeloid lineage. At the same time, deregulation of *SPI1*, *IRF8*, and *KLF4* and upregulation of *MYC* further inhibits differentiation,[30] leading to blast cell accumulation (Figure 5E). This model emphasizes that multiple oncogenic alterations, impacting several signaling pathways, act cooperatively in the etiology of FGFR1-related neoplasms. The proposed model may explain why FGFR1-related neoplasm patients are resistant to all the current therapeutic regimens that have been used to treat acute lymphoblastic leukemia, AML, and other MPN.[1] Thus, this may explain why this disease is largely incurable, although the FGFR1 fusion kinase constitutes a potential therapeutic target. Our analysis suggests that simultaneously targeting FGFR1 signaling as well as multiple other signaling pathways will be essential in developing a successful regimen for future therapy.

Of significant interest is whether FGFR1-related neoplasms are a mixed myeloid and lymphoid (most commonly with T-lymphoid lineage) disorder or represent 2 separate malignancies occurring in 1 patient. Patients with the ZMYM2-FGFR1 fusion carried the rearrangement in both lymphoid and myeloid lineages, suggesting an origin in a common progenitor or stem cell.[31,32] It is also hypothesized that FGFR1-related neoplasms arises from either a common pluripotent stem cell or from a T-cell precursor that retains the potential for myeloid differentiation.[33] Our observations in the syngeneic model showed that, following transplantation in 1 mouse, the initial myeloid lineage disease (AML) shifted to T-lymphoblastic lymphoma (supplemental Figure 3B), suggesting either the presence of leukemia stem cells with T-lymphoid potential, which predominated in the second transplant recipients, or that CNTRL-FGFR1–transformed cells underwent a lineage switch, possibly induced by the internal microenvironment in different recipients, which has been reported in a human model of MLL-AF9 leukemia.[34] The apparent lineage switch does not seem to be derived from emergence of a rare, more aggressive clone, because *Tcrb* rearrangements in cells from both the primary and secondary

transplants showed the same rearrangement pattern (supplemental Figure 3C), indicating that both the AML and T-cell leukemia/lymphomas were derived from the same original clone. Lineage switching from AML to acute lymphoblastic leukemia is extremely rare, with only 2 cases reported.[35,36] The exact molecular mechanism for the lineage conversion is still unknown. However, clonal analysis of lympho-hematopoietic cells in fetal mice has shown the existence of bipotent myeloid-T and myeloid-B lineage progenitors, in addition to multipotent and unipotent progenitors,[37] suggesting a myeloid-based model of hematopoiesis[38,39] in which the stem cell initially generates common myelo-erythroid progenitors and common myelo-lymphoid progenitors. T- and B-cell progenitors subsequently arise from common myelolymphoid progenitors through myeloid-T and myeloid-B stages, respectively. Our studies support this bipotent progenitor model of the myeloid-T theory, evidenced by clonal analysis (supplemental Figure 3) and gene expression profiles (Figure 5C).

The NSG strain is deficient in mature lymphocytes and natural killer cells and is reportedly resistant to lymphoma development.[40] Surprisingly, therefore, we observed enlarged lymph nodes and CD4^{+}/CD8^{+} T-cell leukemia/lymphoma in 2 CTNRL-FGFR1 mice (Figure 6C and supplemental Table 3), which is consistent with our previous conclusion that T-cell leukemia/lymphoma induced by ZMYM2-FGFR1 is independent of thymus function.[12] These results argue against NSG strains being unable to support T-lymphopoiesis after receiving transplants with human cells[41] and supports other observation of human HSC engraftment in NSG mice.[40,42] As such, the NSG model can be used to study leukemogenesis in myeloid and T- and B-lymphoid lineages.

In conclusion, we demonstrate that the CNTRL-FGFR1 fusion kinase induces bilineage myeloid and T-lymphoid disease in both the murine BM transplantation mouse model and, using transduced human CD34^{+} progenitors, in the NSG model with many clinical features similar to human CNTRL-FGFR1. Genetic and molecular analyses in these models demonstrated that multiple signaling pathways, specifically related to myeloid and T-lymphoid lineages, were altered in FGFR1-related neoplasms, which underscores the importance of developing therapies that target all of these signaling pathways to eradicate the leukemia-initiating-cells.

Authorship

Contribution: M.R. and J.K.C. designed the study; M.R., H.Q., and E.K. carried out experiments; and M.R. and J.K.C. wrote the paper.

Conflict-of-interest disclosure: The authors declare no competing financial interests.

Correspondence: Mingqiang Ren, CN2125, Georgia Regents University Cancer Center, 1120 15th St, Augusta, GA 30912; e-mail: mren@gru.edu.

References

1. Jackson CC, Medeiros LJ, Miranda RN. 8p11 myeloproliferative syndrome: a review. *Hum Pathol.* 2010;41(4):461-476.

2. Chen J, Deangelo DJ, Kutok JL, et al. PKC412 inhibits the zinc finger 198-fibroblast growth factor receptor 1 fusion tyrosine kinase and is active in treatment of stem cell myeloproliferative disorder. *Proc Natl Acad Sci USA.* 2004;101(40):14479-14484.

3. Ren M, Li X, Cowell JK. Genetic fingerprinting of the development and progression of T-cell lymphoma in a murine model of atypical myeloproliferative disorder initiated by the ZNF198-fibroblast growth factor receptor-1 chimeric tyrosine kinase. *Blood.* 2009;114(8):1576-1584.

4. Ren M, Tidwell JA, Sharma S, Cowell JK. Acute progression of BCR-FGFR1 induced murine B-lympho/myeloproliferative disorder suggests involvement of lineages at the pro-B cell stage. *PLoS ONE.* 2012;7(6):e38265.

5. Roumiantsev S, Krause DS, Neumann CA, et al. Distinct stem cell myeloproliferative/T lymphoma syndromes induced by ZNF198-FGFR1 and BCR-FGFR1 fusion genes from 8p11 translocations. *Cancer Cell.* 2004;5(3):287-298.

6. Hu S, He Y, Zhu X, Li J, He H. Myeloproliferative disorders with t(8;9)(p12;q33): a case report and review of the literature. *Pediatr Hematol Oncol.* 2011;28(2):140-146.

7. Park TS, Song J, Kim JS, et al. 8p11 myeloproliferative syndrome preceded by t(8;9)(p11;q33), CEP110/FGFR1 fusion transcript: morphologic, molecular, and cytogenetic characterization of myeloid neoplasms associated with eosinophilia and FGFR1 abnormality. *Cancer Genet Cytogenet.* 2008;181(2):93-99.

8. Post GR, Holloman D, Christiansen L, Smith J, Stuart R, Lazarchick J. Translocation t(3;8;9)(p25;p21;q34) in a patient with features of 8p11 myeloproliferative syndrome: a unique case and review of the literature. *Leuk Res.* 2010;34(11):1543-1544.

9. Yamamoto K, Kawano H, Nishikawa S, Yakushijin K, Okamura A, Matsui T. A biphenotypic transformation of 8p11 myeloproliferative syndrome with CEP1/FGFR1 fusion gene. *Eur J Haematol.* 2006;77(4):349-354.

10. Williams DA, Tao W, Yang F, et al. Dominant negative mutation of the hematopoietic-specific Rho GTPase, Rac2, is associated with a human phagocyte immunodeficiency. *Blood.* 2000;96(5):1646-1654.

11. Ren M, Qin H, Ren R, Cowell JK. Ponatinib suppresses the development of myeloid and lymphoid malignancies associated with FGFR1 abnormalities. *Leukemia.* 2013;27(1):32-40.

12. Ren M, Cowell JK. Constitutive Notch pathway activation in murine ZMYM2-FGFR1-induced T-cell lymphomas associated with atypical myeloproliferative disease. *Blood.* 2011;117(25):6837-6847.

13. Deshpande AJ, Cusan M, Rawat VP, et al. Acute myeloid leukemia is propagated by a leukemic stem cell with lymphoid characteristics in a mouse model of CALM/AF10-positive leukemia. *Cancer Cell.* 2006;10(5):363-374.

14. Yamamoto S, Ebihara Y, Mochizuki S, et al. Letter to the Editor: quantitative PCR detection of CEP110-FGFR1 fusion gene in a patient with 8p11 syndrome. *Leuk Lymphoma.* 2013;Feb. 16.

15. Mandel EM, Grosschedl R. Transcription control of early B cell differentiation. *Curr Opin Immunol.* 2010;22(2):161-167.

16. Santos PM, Borghesi L. Molecular resolution of the B cell landscape. *Curr Opin Immunol.* 2011;23(2):163-170.

17. Mombaerts P, Mizoguchi E, Grusby MJ, Glimcher LH, Bhan AK, Tonegawa S. Spontaneous development of inflammatory bowel disease in T cell receptor mutant mice. *Cell.* 1993;75(2):274-282.

18. Philpott KL, Viney JL, Kay G, et al. Lymphoid development in mice congenitally lacking T cell receptor alpha beta-expressing cells. *Science.* 1992;256(5062):1448-1452.

19. Palomero T, Sulis ML, Cortina M, et al. Mutational loss of PTEN induces resistance to NOTCH1 inhibition in T-cell leukemia. *Nat Med.* 2007;13(10):1203-1210.

20. Doulatov S, Notta F, Laurenti E, Dick JE. Hematopoiesis: a human perspective. *Cell Stem Cell.* 2012;10(2):120-136.

21. Feinberg MW, Wara AK, Cao Z, et al. The Kruppel-like factor KLF4 is a critical regulator of monocyte differentiation. *EMBO J.* 2007;26(18):4138-4148.

22. Laiosa CV, Stadtfeld M, Graf T. Determinants of lymphoid-myeloid lineage diversification. *Annu Rev Immunol.* 2006;24:705-738.

23. Rosenbauer F, Tenen DG. Transcription factors in myeloid development: balancing differentiation with transformation. *Nat Rev Immunol.* 2007;7(2):105-117.

24. Luo H, Li Q, O'Neal J, Kreisel F, Le Beau MM, Tomasson MH. c-Myc rapidly induces acute myeloid leukemia in mice without evidence of lymphoma-associated antiapoptotic mutations. *Blood.* 2005;106(7):2452-2461.

25. Stirewalt DL, Radich JP. The role of FLT3 in haematopoietic malignancies. *Nat Rev Cancer.* 2003;3(9):650-665.

26. van der Meer LT, Jansen JH, van der Reijden BA. Gfi1 and Gfi1b: key regulators of hematopoiesis. *Leukemia.* 2010;24(11):1834-1843.

27. O'Hare T, Shakespeare WC, Zhu X, et al. AP24534, a pan-BCR-ABL inhibitor for chronic myeloid leukemia, potently inhibits the T315I mutant and overcomes mutation-based resistance. *Cancer Cell.* 2009;16(5):401-412.

28. Delmore JE, Issa GC, Lemieux ME, et al. BET bromodomain inhibition as a therapeutic strategy to target c-Myc. *Cell.* 2011;146(6):904-917.

29. Zhou L, Fu W, Yuan Z, Hou J. Complete molecular remission after interferon alpha treatment in a case of 8p11 myeloproliferative syndrome. *Leuk Res.* 2010;34(11):e306-e307.

30. Hoffman B, Amanullah A, Shafarenko M, Liebermann DA. The proto-oncogene c-myc in hematopoietic development and leukemogenesis. *Oncogene.* 2002;21(21):3414-3421.

31. Inhorn RC, Aster JC, Roach SA, et al. A syndrome of lymphoblastic lymphoma, eosinophilia, and myeloid hyperplasia/malignancy associated with t(8;13)(p11;q11): description of a distinctive clinicopathologic entity. *Blood.* 1995;85(7):1881-1887.

32. Macdonald D, Aguiar RC, Mason PJ, Goldman JM, Cross NC. A new myeloproliferative disorder associated with chromosomal translocations involving 8p11: a review. *Leukemia.* 1995;9(10):1628-1630.

33. Vega F, Medeiros LJ, Davuluri R, Cromwell CC, Alkan S, Abruzzo LV. t(8;13)-positive bilineal lymphomas: report of 6 cases. *Am J Surg Pathol.* 2008;32(1):14-20.

34. Wei J, Wunderlich M, Fox C, et al. Microenvironment determines lineage fate in a human model of MLL-AF9 leukemia. *Cancer Cell.* 2008;13(6):483-495.

35. Krawczuk-Rybak M, Zak J, Jaworowska B. A lineage switch from AML to ALL with persistent translocation t(4;11) in congenital leukemia. *Med Pediatr Oncol.* 2003;41(1):95-96.

36. Lounici A, Cony-Makhoul P, Dubus P, Lacombe F, Merlio JP, Reiffers J. Lineage switch from acute myeloid leukemia to acute lymphoblastic leukemia: report of an adult case and review of the literature. *Am J Hematol.* 2000;65(4):319-321.

37. Lu M, Kawamoto H, Katsube Y, Ikawa T, Katsura Y. The common myelolymphoid progenitor: a key intermediate stage in hemopoiesis generating T and B cells. *J Immunol.* 2002;169(7):3519-3525.

38. Katsura Y. Redefinition of lymphoid progenitors. *Nat Rev Immunol.* 2002;2(2):127-132.

39. Kawamoto H. A close developmental relationship between the lymphoid and myeloid lineages. *Trends Immunol.* 2006;27(4):169-175.

40. Shultz LD, Lyons BL, Burzenski LM, et al. Human lymphoid and myeloid cell development in NOD/LtSz-scid IL2R gamma null mice engrafted with mobilized human hemopoietic stem cells. *J Immunol.* 2005;174(10):6477-6489.

41. Agerstam H, Järås M, Andersson A, et al. Modeling the human 8p11-myeloproliferative syndrome in immunodeficient mice. *Blood.* 2010;116(12):2103-2111.

42. Risueño RM, Campbell CJ, Dingwall S, et al. Identification of T-lymphocytic leukemia-initiating stem cells residing in a small subset of patients with acute myeloid leukemic disease. *Blood.* 2011;117(26):7112-7120.